JOURNAL OF SOLID STATE CHEMISTRY 44, 382–387 (1982)

Preparation and Properties of PdPSe Single Crystals

JAMES V. MARZIK, ROBERT KERSHAW, KIRBY DWIGHT, AND AARON WOLD*

Department of Chemistry, Brown University, Providence, Rhode Island 02912

Received February 22, 1982; in revised form April 12, 1982

Single crystals of PdPSe were shown to be *n*-type semiconductors. Weak Pauli paramagnetic behavior was observed, which is consistent with the presence of delocalized electrons. Electrical measurements showed a room-temperature resistivity $\rho = 70$ ohm-cm, activation energy of resistivity $E_a = 0.32$ eV, and Hall mobility $\mu = 34$ cm^2 V^{-1} sec^{-1}. Photoelectronic measurements in aqueous solutions of I^-/I_3^- indicate that PdPSe has high quantum efficiencies below 800 nm. The indirect optical band gap is 1.28(2) eV.

Introduction

In recent years several investigators have studied the application of semiconductor electrodes in the construction of photoelectrochemical, photovoltaic, and electrophotosynthetic cells. There are several excellent reviews of these studies (*1–3*). Tributsch *et al.* (*4, 5*) reported the use of MoS_2 and related semiconducting layer-type dichalcogenides in photoelectrochemical cells which show reasonably good efficiencies and long-term stability in aqueous solution, and since then, there have been several investigations of the photoelectrochemical behavior of layer-type transition metal compounds (e.g., *6–8*).

Since PdPSe is a layer-type compound and no semiconducting compound has been reported with a palladium photoactive center, it was of interest to synthesize large single crystals and investigate their magnetic, electrical, optical, and (particularly) photoelectronic properties.

PdPSe was first reported by Bither *et al.* (*9*), and the structure of the isostructural PdPS was determined by Jeitschko (*10*). PdPSe, orthorhombic space group *Pbcn*, has a layer-type structure (Fig. 1) with Pd in square–planar coordination with two Se and two P atoms. Weaker interactions with Se and another Pd atom above and below the coordination plane extend the coordination geometry to an extremely elongated octahedron. Phosphorous is tetrahedrally coordinated to two Pd, one Se, and one P atom. Selenium is tetrahedrally coordinated to two Pd and one P, with the fourth "bond" of the tetrahedron a weak interaction with a Pd atom from another layer. Each layer consists of a net of puckered pentagons which contain either two Pd, two P, and one Se or two Pd, two Se, and one P. Every other layer is connected by strong P–P bonds to form double layers of pentagon nets connected by weak Pd–Se interac-

* To whom all correspondence should be addressed.

0022-4596/82/120382-06$02.00/0

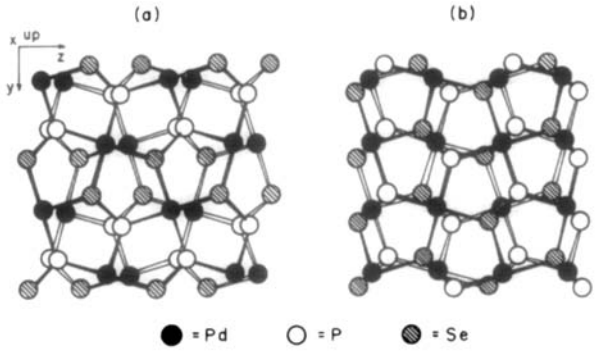

FIG. 1. Relative positions of atomic layers in the PdPSe structure. Atoms in the upper layers are connected by solid lines and those in the lower layers by double lines. The double layers of PdPSe shown in (a) are connected by P–P bonds and weaker Pd–Pd interactions. (b) illustrates the relative positions of two layers (the "top" of one double layer and the "bottom" of another) which are connected by weak Pd–Se interactions.

tions presumably broken upon cleavage of the crystal. Thus, the surface layer contains both Pd and Se atoms. Most CdI_2- or MoS_2-type compounds consist of anion–metal–anion layers loosely bound to one another by van der Waals' forces, which upon cleavage produce anion surfaces. The presence of palladium, a well-known catalyst, on the surface of a photoactive crystal suggests the possibility of photocatalytic reactions.

Experimental

Synthesis. Single crystals of PdPSe were prepared from the elements by vapor sublimation. Palladium (Engelhard 99.99% pure) was prereduced at 900°C under 85%/15% Ar/H_2 gas for 16 hr then heated for 4 hr at 350°C under dynamic vacuum to remove hydrogen. Phosphorus (Leico 99.999% pure) and selenium (Gallard–Schlesinger 99.999% pure) were used as received. Stoichiometric amounts of the elements were sealed in an evacuated silica tube of dimensions 14 mm o.d. × 12 mm i.d. × 28 cm. The tube was placed in a three-zone furnace (the third zone allowing good temperature control in the crystal growth zone), and the charge was prereacted for 24 hr at 600°C, with the growth zone at 1000°C preventing transport of product. The furnace was then equilibrated at 880°C and programmed over 24–48 hr to give a temperature of 850°C in the charge zone and 800°C in the growth zone. Crystal growth took place in 5–7 days. PdPSe formed silver-colored, graphite-like thin rectangular single-crystal platelets ranging from 1 to 50 mm^2 in area and 5–50 μm in thickness. Analysis calculated for PdPSe: Pd, 49.18; P, 14.32. Found: Pd, 49.94, 49.96; P, 15.11, 15.18 (see Ref. (*9*)).

X-Ray analysis. X-Ray diffraction patterns of small single crystals were obtained using a Gandolfi camera (Blake Industries, Model D1100) and Cu$K\alpha$ radiation. Lattice parameters were obtained by least-squares refinement of the diffraction data.

Magnetic measurements. Magnetic susceptibility was measured using a Faraday balance (*11*) over the range from liquid nitrogen to room temperature at a field strength of 10.4 kOe. Honda–Owen plots were also made, and the absence of any field dependency indicated the absence of ferromagnetic impurities. The data were then corrected for core diamagnetism (*12*).

Electrical measurements. Resistivity and DC Hall effect were measured on single crystals using the van der Pauw technique

(*13*). Contacts were made by the ultrasonic soldering of indium directly onto the samples, and ohmic behavior was established by measuring current-voltage characteristics. Activation energy of resistivity, E_a (defined for semiconductors by $\rho = \rho_0 \exp(E_a/kT)$, where ρ = resistivity, ρ_0 is a constant, T = temperature (K), and k = Boltzmann constant), was determined by measuring ρ as a function of T.

Optical measurements. Optical absorption of thin (5–25 μm) single crystals was measured with a Cary 17 spectrophotometer. The absorption coefficient α was calculated from the transmission ratio T using the expression $T = (1 - R)^2 e^{-\alpha t}[1 - R^2 e^{-2\alpha t}]^{-1}$, where t is the sample thickness and R is the reflectivity calculated from the above expression by assuming $\alpha \simeq 0$ in the part of the spectrum far removed from the absorption edge.

Electrode preparation. Photoelectrodes were prepared by evaporating a thin film of gold on the back of the single crystals of PdPSe in order to provide good electrical contact. For mechanical support, the crystal was affixed to a disk of platinum foil with a drop of silver paint. The platinum foil was soldered to the platinum electrode wire which was sealed inside a Pyrex tube. An insulating resin (Miccrostop, Michigan Chrome Chemical Corp.) was applied to the platinum foil and wire so that only the front surface of the crystal was in electrical contact with the electrolyte solution.

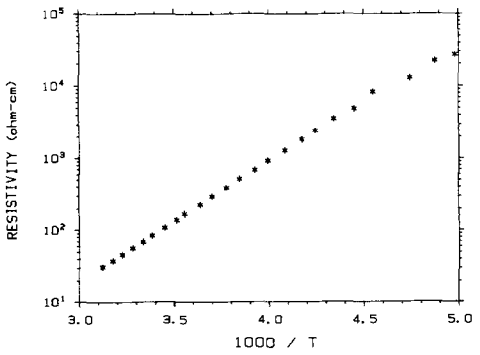

FIG. 2. Resistivity of PdPSe plotted as a function of temperature.

TABLE I

ELECTRICAL PROPERTIES OF PdPSe

	ρ^a (ohm-cm)	E_a (eV)	n (cm^{-3})	μ_H ($cm^2\ V^{-1}\ sec^{-1}$)
This work	70	0.32[b]	2.4×10^{15}	34
Literature[d]	30	0.15[c]	—	—

[a] 300K.
[b] 200–320K.
[c] 300–400K.
[d] Ref. (*9*).

Photoelectronic measurements. Photoelectronic measurements were carried out with a 150-W xenon lamp, a monochromator (Oriel Model 7240), a glass cell with a quartz window, and a current amplifier as previously described (*14*). A tungsten iodide lamp was used for wavelength dependency measurements. The quantum efficiency η was determined by dividing the current through the cell by the incident photon flux, measured with a calibrated Si photodiode. The electrolyte used was an aqueous solution of 0.05 *M* NaI/0.002 *M* I_2/0.05 *M* H_2SO_4. This most likely results in the I^-/I_3^- couple as the electroactive species in solution (*6*). The electrolyte was purged of dissolved oxygen by continuous bubbling of nitrogen gas. At 0.0 V bias with respect to the counter electrode, the potential of the working electrode was 0.335 V versus SCE.

Results and Discussion

X-Ray analysis shows that PdPSe has orthorhombic diffraction symmetry. Cell dimensions $a = 13.59(3)$, $b = 5.81(1)$, and $c = 5.85(1)$ Å, obtained by least-square refinement of Gandolfi X-ray data, agree well with those obtained by Bither *et al.* (*9*).

The electrical properties of PdPSe are summarized in Fig. 2 and Table I. This material is a semiconductor with a room-tem-

perature resistivity of 70 ohm-cm and an activation energy of resistivity of 0.32 eV. DC Hall and Seebeck measurements show that the sign of the majority carrier is negative, which is indicative of an n-type semiconductor. Hall measurements indicate a relatively low concentration of charge carriers (2.4×10^{15} cm^{-3}) with moderately high mobility (34 cm^2 V^{-1} sec^{-1}). These measurements were restricted to the basal plane because of the thinness of the crystals.

It can be seen from the magnetic data shown in Fig. 3 that PdPSe is Pauli paramagnetic; this is indicative of some electron delocalization, consistent with the low resistivity.

The photoresponse observed for PdPSe is shown in Fig. 4, where the photocurrents obtained in "white" light are plotted against the anode potential measured with respect to a saturated calomel electrode (SCE). The onset of the photocurrent indicates a flat-band potential of approximately 0.1 V vs SCE. Anodic dark current was negligible (0–0.05 mA/cm^2) compared to the observed anodic photocurrent. When the PdPSe electrode was biased cathodically (with respect to the counter electrode), a somewhat higher cathodic dark current (0–1 mA/cm^2) was observed due to the diode character of the semiconductor–electrolyte junction. The photocurrent is

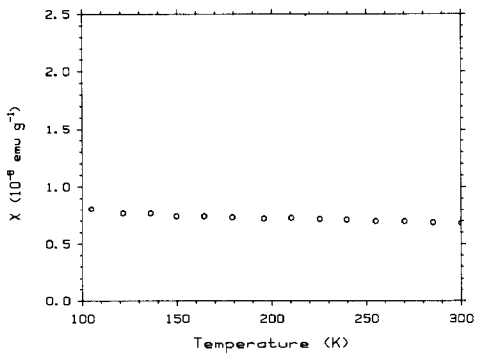

FIG. 3. Magnetic susceptibility of PdPSe plotted as a function of temperature.

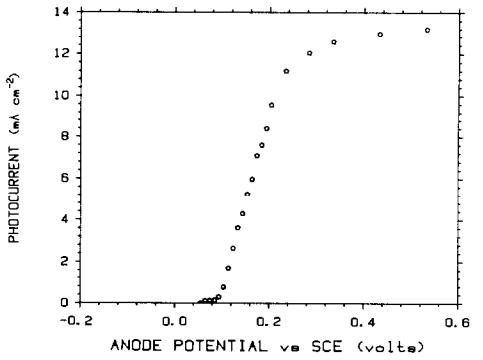

FIG. 4. Variation of photocurrent with anode potential under "white" xenon arc irradiation of 1.0 W/cm^2 in 0.05 M NaI/0.002 M I_2/0.05 M H_2SO_4 electrolyte solution.

due to the reversible oxidation of I^- to I_3^- (or I_2), since a cell containing only 0.05 M H_2SO_4 as the electrolyte showed negligible photocurrent.

The quantum efficiency η (in electrons/photon) measured at an anode potential of 0.335 V vs SCE is plotted vs wavelength in Fig. 5. Experiments showed negligible electrolyte absorption in this spectral region. The onset of photocurrent corresponds very closely to the absorption edge of 960 nm measured from the optical absorption spectrum. There is a steady increase in η with decreasing wavelength until it levels off at about 60% at 600 nm. This value is not corrected for reflectance. The reflectivity of 0.37 was calculated from the absorption spectrum. Correcting for reflectivity results in quantum efficiencies of 90–100% below 600 nm. Below 530 nm, the quantum efficiency decreases somewhat, a phenomenon observed for other layer-type materials (*4–7, 15*).

It has been suggested (*5, 15*) that the photoeffect observed in layer-type transition metal dichalcogenides is due to d–d electron transitions. Such a model would be consistent with the observed decrease in photocurrent at the shorter wavelengths, the electrical properties, and stability. The electron delocalization, indicative of d-or-

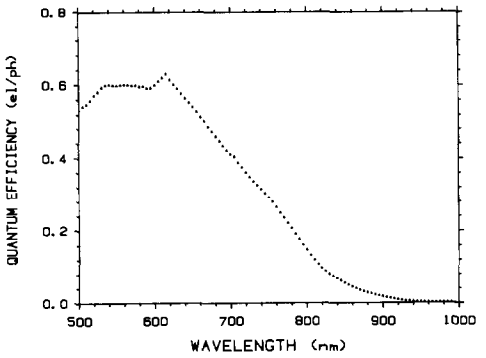

FIG. 5. Spectral variation of the quantum efficiency obtained at an anode potential of 0.335 V vs SCE in 0.05 *M* NaI/0.002 *M* I_2/0.05 *M* H_2SO_4.

bital conduction, is evidenced by the Pauli paramagnetism and the moderately high mobility (see Table I). The PdPSe photoelectrodes were used reproducibly for several experiments. This stability suggests that the photoeffect is due to $d-d$ transitions rather than the breaking of metal–anion bonds. A similar model has been proposed by Tributsch for the stability of the layered dichalcogenides (*4*).

Analysis of the spectral response data can yield values for various energy transitions (*16*). Accordingly, the quantity $(\eta h\nu)^{0.5}$ plotted as a function of the photon energy (Fig. 6) yields a lowest-energy indirect optical band gap of 1.28(1) eV. This is in good agreement with the band gap obtained by analyzing the optical absorption spectrum. Figure 7 is a plot of $(\alpha h\nu)^{0.5}$ as a function of photon energy, which results in a lowest-energy indirect optical band gap of 1.29(1) eV. From the sudden increase in slope present in Fig. 6, a higher energy band transition at 1.48(5) eV can be estimated.

Summary and Conclusions

Large single crystals of PdPSe were grown by vapor sublimation and several of their properties were investigated. PdPSe was found to be an *n*-type semiconductor with weak Pauli paramagnetic behavior. DC Hall measurements indicate a low concentration of highly mobile charge carriers. Photoelectronic measurements show PdPSe to be a photoactive material with high quantum efficiencies below 800 nm. Optical and photoelectronic measurements agree closely, giving a lowest-energy indirect optical band gap of 1.28(2) eV. Analysis of the photoelectronic spectral response also results in a measured higher-energy indirect transition at 1.48(5) eV.

Because of its unique layer structure, the surface of the natural cleavage plane of a PdPSe crystal contains both Pd and Se atoms. Since palladium is present at the cleavage plane of this photoactive material,

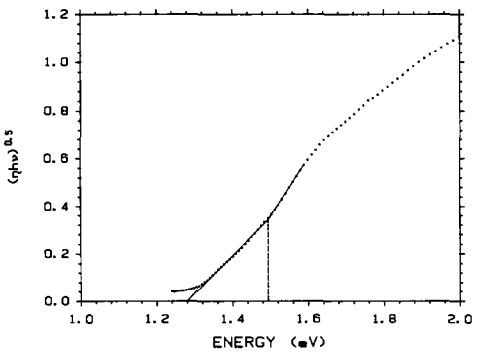

FIG. 6. Indirect band gap analysis for PdPSe showing transitions at 1.28(1) and 1.48(5) eV.

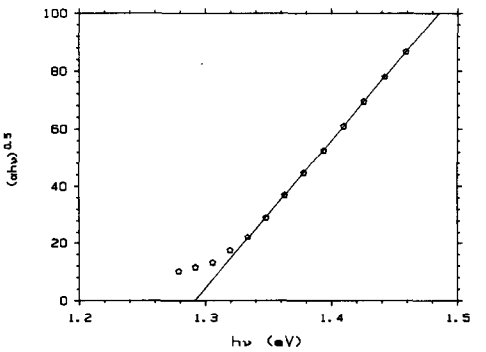

FIG. 7. Analysis of the optical absorption spectrum of PdPSe in the region of the absorption edge, giving a lowest energy-indirect optical band gap of 1.29(1) eV.

there is the possibility that this or similar palladium-containing photoactive materials may provide surfaces on which photocatalytic reactions can take place.

Acknowledgments

The authors would like to thank GTE Laboratories, Inc., of Waltham, Massachusetts, for the support of James V. Marzik. Acknowledgment is also made to the National Science Foundation (DMR-82–03667) for the support of Kirby Dwight. In addition, the authors would like to acknowledge the support of the Materials Research Laboratory Program at Brown University.

References

1. A. J. Nozik, *Annu. Rev. Phys. Chem.* **29,** 189 (1978).
2. M. S. Wrighton, *Acc. Chem. Res.* **12,** 303 (1979).
3. A. J. Bard, *Science* **207,** 139 (1980).
4. H. Tributsch and J. C. Bennett, *J. Electroanal. Chem.* **81,** 97 (1977).
5. H. Tributsch, *J. Electrochem. Soc.* **125,** 1086 (1978).
6. F. F. Fan, H. S. White, B. L. Wheeler, and A. J. Bard, *J. Amer. Chem. Soc.* **102,** 5142 (1980).
7. H. J. Lewerenz, A. Heller, and F. J. Disalvo, *J. Amer. Chem. Soc.* **102,** 1877 (1980).
8. L. F. Schneemeyer and M. S. Wrighton, *J. Amer. Chem. Soc.* **101,** 6496 (1979).
9. T. A. Bither, P. C. Donohue, and H. S. Young, *J. Solid State Chem.* **3,** 300 (1971).
10. W. Jeitschko, *Acta Crystallogr. Sect. B* **30,** 2565 (1974).
11. B. Morris and A. Wold, *Rev. Sci. Instrum.* **39,** 1937 (1968).
12. P. W. Selwood, "Magnetochemistry," 2nd ed., Interscience, New York (1956).
13. L. J. van der Pauw, *Philips Res. Rep.* **13,** 1 (1958).
14. S. N. Subbarao, Y. H. Yun, R. Kershaw, K. Dwight, and A. Wold, *Mater. Res. Bull.* **13,** 1461 (1978).
15. J. Gobrecht, H. Gerischer, and H. Tributsch, *Ber. Bunsenges. Phys. Chem.* **82,** 1331 (1978).
16. F. P. Koffyberg, K. Dwight, and A. Wold, *Solid State Commun.* **30,** 433 (1979).